Annals of Anatomy 205 (2016) 60–64

Contents lists available at ScienceDirect

Annals of Anatomy

journal homepage: www.elsevier.com/locate/aanat

Research article

Anatomy of the true interatrial septum for transseptal access to the left atrium

Wiesława Klimek-Piotrowska [1], Mateusz K. Hołda [*,1], Mateusz Koziej, Katarzyna Piątek, Jakub Hołda

Department of Anatomy, Jagiellonian University Medical College, Cracow, Poland

ARTICLE INFO

Article history:
Received 6 January 2016
Received in revised form 23 January 2016
Accepted 25 January 2016

Keywords:
Transseptal puncture
Septal pouch
Patent foramen ovale
Fossa ovalis

ABSTRACT

Clinical anatomy of the interatrial septum is treacherous, difficult and its unfamiliarity can cause many serious complications. This work aims to create an anatomical map of the true interatrial septum. An appreciation of the anatomical situation is essential for safe and efficacious transseptal access from the right atrium to the left heart chambers. Examination of 135 autopsied human hearts (Caucasian) of both sexes (28% females) aged from 19 to 94 years old (47.0 ± 18.2) with BMI = 27.1 ± 6.0 kg/m^2 was conducted. Focus was specifically targeted on the assessment of the fossa ovalis, patent foramen ovale (PFO), and right-sided septal pouch (RSP) morphology. Mean values of cranio-caudal and antero-posterior fossa ovalis diameters were 12.1 ± 3.6 and 14.1 ± 3.6 mm, respectively. The fossa ovalis was situated an average of 10.1 ± 4.4 mm above the inferior vena cava ostium, 20.7 ± 5.2 mm from the right atrioventricular ring, and 12.6 ± 5.2 mm under the right atrium roof. Four types of fossa ovalis anatomy have been observed (smooth-56.3%, PFO-24.4%, RSP-11.9%, net-like formation-7.4%). The PFO mean channel length was 10.5 ± 5.2 mm. The tunnel-like PFO (channel length ≥12 mm) was observed in 8.9% of specimens. The RSP was observed in 11.9% of specimens (with mean depth = 6.3 ± 3.8 mm) and was directed apex upward in all observed specimens (may imitate the PFO channel). The fossa ovalis/interatrial septum surface area ratio was 18.3 ± 9.0%. In conclusion: (1) An anatomical map of the interatrial septum from the right atrial side was presented. (2) The RSP may imitate the PFO channel. (3) The "true" interatrial septum represents only about 20% of the whole interatrial septum area. (4) There is wide variation in the location and geometry of the fossa ovalis. (5) We could distinguish four different types of the fossa ovalis area.

1. Introduction

It has been over half a century since Ross, Braunwald, and Morrow provided the first description of the transseptal left atrial puncture technique, which permits a direct route to the left atrium via the systemic venous system, right atrium and interatrial septum (Ross et al., 1960). Prior to this development, obtaining percutaneous access to the left atrium was one of the most difficult cardiac procedures. The left atrium was commonly reached by retrograde arterial cannulation via the left ventricle and mitral valve, although the manipulation of catheters proved problematic due to multiple required 90° turns (Zimmerman et al., 1950). Alternative techniques, such as: transbronchial (Facquet et al., 1952), transthoracic (Bjork et al., 1953), suprasternal (Radner, 1954) and direct ventricular (Brock et al., 1956) puncture have been proposed, but each has certain disadvantages. Another method of left atrial access utilized natural connections between the right and left atria, such as a patent foramen ovale (PFO) or other atrial septal defects. This access was new, still developed, and limited to a small number of patients with favorable anatomical conditions. Brockenbrough (Brockenbrough et al., 1962), and later Mullins (Mullins, 1983) refined the transseptal puncture procedure with several critical modifications. Today, both transseptal puncture and access through PFO are widely used cardiac techniques. Transseptal access is commonly employed during the following procedures: catheter ablation, pulmonary vein isolation, left atrial appendage closure, PFO and atrial septal defect repair, percutaneous mitral valvuloplasty, MitraClip catheter-based mitral valve repair, hemodynamic assessment of the mitral valve, paravalvular leak closure, and as

* Corresponding author at: Department of Anatomy Jagiellonian University Medical College Kopernika 12, 31-034 Kraków, Poland. Tel.: +48 124229511; fax: +48 124229511.
E-mail address: mkh@onet.eu (M.K. Hołda).
[1] These authors contributed equally.

http://dx.doi.org/10.1016/j.aanat.2016.01.009
0940-9602/

an alternative access to the left ventricle in the presence of a prosthetic aortic valve (Earley, 2009; Jönsson and Settergren, 2010). For experienced operators, it is usually an uncomplicated procedure, however, in some cases it may be extremely difficult, with fatal complications (Katritsis et al., 2013).

An appreciation of the anatomical conditions is essential for safe and efficacious transseptal access from the right atrium to the left heart chambers. Clinical anatomy of the true interatrial septum is treacherous, difficult and its unfamiliarity can cause many serious complications. Thus, the aim of our study was to assess the regional morphology of the right atrium and interatrial septum for a deeper understanding.

2. Materials and method

The study was designed and conducted by the Department of Anatomy, Jagiellonian University Medical College in Cracow, Poland and approved by the Bioethical Committee of the Jagiellonian University Medical College, Cracow (KBET/51/B/2013).

Heart specimens were collected during routine forensic medical autopsies performed at the Department of Forensic Medicine, Jagiellonian University Medical College from July 2013 to October 2014. The hearts were removed together with the proximal portions of the great vessels: the ascending aorta, pulmonary trunk, superior vena cava (SVC), inferior vena cava (IVC), and all pulmonary veins. All specimens were randomly selected. Exclusion criteria include: severe anatomical defects, states after operations and grafts on the heart, obvious severe macroscopic pathology of the heart or vascular system found during the autopsy (aneurysms, storage diseases), heart trauma, and macroscopic signs of decomposition of cadavers. Other conditions such as: myocardial infarction, arterial and pulmonary hypertension, cardiomyopathy, heart failure, arrhythmias were not recognized as an exclusion criteria. After dissection all hearts were fixed in 10% paraformaldehyde for a maximum of 2 months until the time of measurement.

Our study included 135 randomly selected adult human hearts (Caucasian) of both sexes (28% females) aged from 19 to 94 years old (47.0 ± 18.2) with an average measured body mass index (BMI) of $27.1 \pm 6.0\ kg/m^2$. All specimens were opened in a common manner. The right atrium was opened by an incision extending from the orifice of the SVC to the orifice of the IVC. The Eustachian valve associated with the orifice of the IVC however was not sectioned. The left atrium was opened by an incision extending between associated pairs of left and right pulmonary veins.

All descriptions and measurements were undertaken with the heart held in anatomical position. All measurements were conducted by 0.03 mm precision electronic caliper YATO (YT–7201). In order to reduce human error, two researchers obtained measurements. If the measurements of one parameter differed by more than 10% then they were not included in the database and the sample was measured again. The mean of the two measurements was calculated, rounding to the tenths decimal place. The following measurements were made: the shortest distance between the IVC and SVC ostia; width of the interatrial septum from the right atrium side (the longest antero-posterior diameter); cranio-caudal and antero-posterior diameters of the fossa ovalis as the largest lengths between opposite sides of the limbus of the fossa ovalis; and the shortest distances from the limbus of the fossa ovalis to the right atrioventricular ring, to the IVC ostium, and to the right atrium roof. The greatest distance from the limbus fossae ovalis to the edge of the infero-anterior rim (to the nearest point were the needle does not pass directly from the right to the left atrium) was measured. The approximate surface area of the fossa ovalis and the interatrial septum as well as the ratio of the fossa ovalis surface area to the entire interatrial septum surface area were calculated.

The appearance, location and morphology of the fossa ovalis, PFO, right-sided septal pouch (RSP), and muscle bridges within the right atrium were assessed. The positions of PFO and RSP orifices within the fossa ovalis were noted and the length of the PFO channel and RSP depth were measured. The floor of the fossa ovalis was transluminated from the left atrial side.

Hearts were weighed prior to paraformaldehyde treatment. The heart circumference defined as the smallest circumference of the heart at the atrio-ventricular groove (coronary grove) was obtained, and measurements of other main heart structures were performed to determine the presence of additional relative anatomic relationships.

Data are presented as mean values and corresponding standard deviations. StatSoft Statistica 10.0 for Windows was used for all statistical analyses. *P*-values less than 0.05 were considered to be statistically significant. Correlation coefficients were calculated to measure statistical dependence and the Student's *t*-tests and Mann–Whitney *U*-tests were performed for statistical comparisons.

3. Results

Minimum, maximum, median, and mean values with standard deviations of obtained anatomical measurements and calculations are presented in Table 1. The map of the interatrial septum from the right atrial side is shown in Fig. 1. The distance between the IVC and SVC ostia showed an increase with age ($r = 0.36$; $p = 0.00$), BMI ($r = 0.35$; $p = 0.00$), heart weight ($r = 0.39$; $p = 0.00$), heart circumference ($r = 0.28$; $p = 0.002$), IVC diameter ($r = 0.24$; $p = 0.006$), and cross-sectional area of the right atrioventricular ring ($r = 0.21$; $p = 0.01$). The interatrial septum width also showed an increase with age ($r = 0.27$; $p = 0.001$) and heart circumference ($r = 0.18$; $p = 0.04$).

The fossa ovalis is an oval or round depression in the lower posterior part of the interatrial septum and is composed primarily of thin fibrous tissue. It was oval in 55.6% and round in 44.4% of cases. The calculated ratio of the fossa ovalis surface area to the entire interatrial septum surface area was correlated with the heart weight ($r = 0.27$; $p = 0.002$). Mean values of cranio-caudal and antero-posterior fossa ovalis diameters were higher in heavier hearts ($r = 0.30$; $p = 0.001$ and $r = 0.21$; $p = 0.028$), and increased with age ($r = 0.234$; $p = 0.015$ and $r = 0.34$; $p = 0.000$, respectively). Cranio-caudal diameter also showed an increase with IVC diameter ($r = 0.28$; $p = 0.001$), while the antero-posterior diameter showed a direct correlation with diameter ($r = 0.19$; $p = 0.03$) and cross-sectional area ($r = 0.24$; $p = 0.005$) of right atrioventricular ring and IVC diameter ($r = 0.17$; $p = 0.04$). The fossa ovalis area was increased with age ($r = 0.2$; $p = 0.018$). The distance between the fossa ovalis limbus and the right atrium roof was increased with BMI ($r = 0.2$; $p = 0.017$), age ($r = 0.19$; $p = 0.025$), and heart circumference ($r = 0.28$; $p = 0.0015$). The sex showed no influence on any above-mentioned parameters.

The PFO (Fig. 2b) was present in 24.4% with a mean channel length of 10.5 ± 5.2 mm. The tunnel-like PFO (channel length $\geq$12 mm) was observed in 8.9% of all cases (36.4% of PFO cases). The PFO channel was directed superiorly and anteriorly in all observed cases. PFO channel length showed an inverse correlation with BMI ($r = -0.38$; $p = 0.034$) and increased with the length of the left atrial appendage ($r = 0.38$; $p < 0.05$). The PFO orifice was primarily located in the superior-central circumference of the fossa ovalis (78.8% of cases), and secondarily within the superior-posterior circumference of the fossa ovalis (21.2%). The frequency of PFO occurrence was higher in young adults than in elderly people ($p = 0.005$).

The septal pouch is defined as an invaginated portion of the septum formed in the absence of the PFO channel as a result of incomplete fusion of the embryological components of the

Table 1
Results of obtained anatomical measurements and calculations.

Name	*N*	Minimum	Maximum	Median	Mean	SD
Heart weight (g)	135	150.0	780.0	448.0	451.5	113.7
Distance between ICV and SVC ostia (mm)	135	17.0	62.0	34.0	35.0	7.3
Interatrial septum width (mm)	135	12.8	62.0	28.6	29.3	8.1
FO CD (mm)	135	3.8	26.9	12.0	12.1	3.6
FO AP (mm)	135	4.9	24.3	14.0	14.1	3.6
FO area (mm^2)	135	9.2	424.3	136.9	142.7	65.0
Fossa ovalis/Interatrial septum-Ratio (%)	135	2.9	51.5	17.6	18.3	9.0
LR (mm)	135	7.0	30.4	21.1	20.7	5.2
LO (mm)	135	2.9	28.0	8.9	10.1	4.4
LS (mm)	135	4.0	28.0	12.0	12.6	5.2
RIM (mm)	135	1.1	11.2	3.8	4.4	2.4
PFO channel length (mm)	33	4.2	15.6	10.4	10.5	3.2
RSP depth (mm)	16	3.0	17.1	5.0	6.3	3.8

N – number of hearts; FO – fossa ovalis; FO AP – anteroposterior fossa ovalis diameter; FO CD – craniocaudal fossa ovalis diameter; IVC – inferior vena cava; LO – the distance from the limbus of the fossa ovalis to the inferior vena cava ostium; LR – the distance from the limbus of the fossa ovalis to the right atrioventricular ring; LS – the distance from the limbus of the fossa ovalis to the right atrium roof; PFO – patent foramen ovale; RIM – distance from the limbus fossae ovalis to the edge of the infero-anterior rim; RSP – right-sided septal pouch; SD – standard deviations; SVC – superior vena cava.

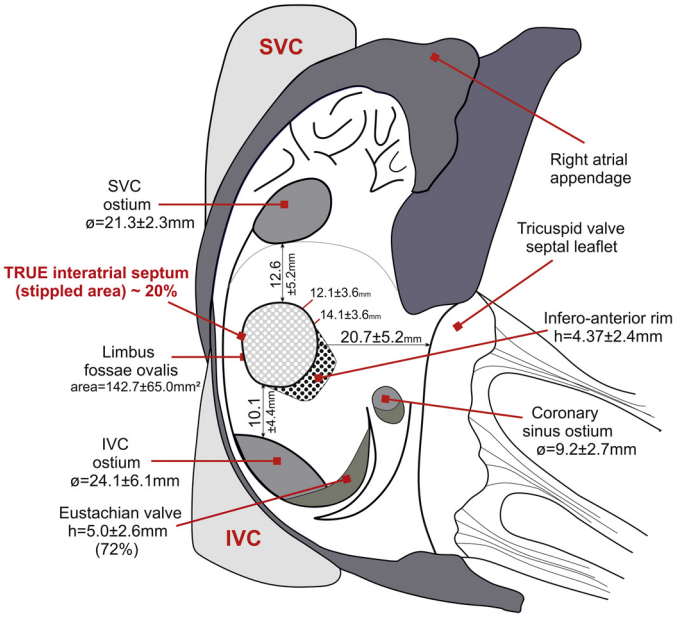

Fig. 1. The right atrium scheme. The view of interatrial septum from the right atrial side (mean values). Stippled area represents the true interatrial septum. IVC – inferior vena cava; SVC – superior vena cava.

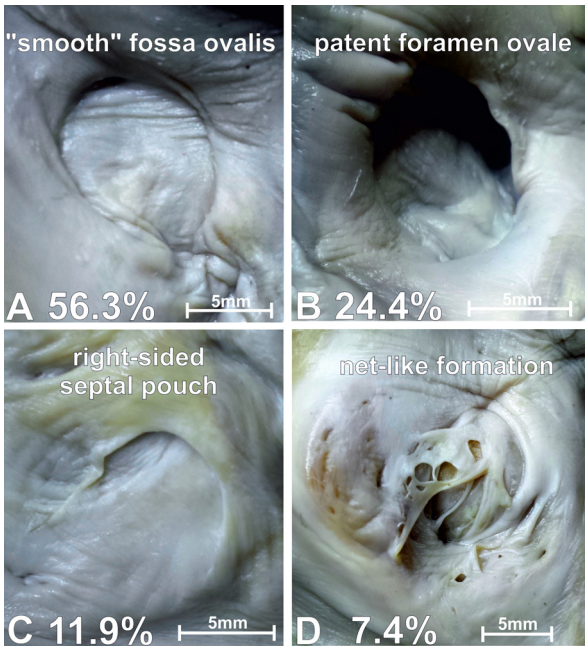

Fig. 2. Photographs of cadaveric heart specimens showing four different types of fossa ovalis anatomy. A – "smooth" fossa ovalis; B – patent foramen ovale; C – right-sided septal pouch (blindly ending pocket within interatrial septum which is opened into right atrium); D – net-like formation within the fossa ovalis.

interatrial septum (Krishnan and Salazar, 2010). In this study, a septal pouch opening to the right atrium was observed in 11.9% of specimens (Fig. 2c). The apex of the RSP was observed in a superiorly directed orientation in all specimens. The most common location of the RSP orifice was as follows: superior-anterior (62.5%), superior-central (25%), superior-posterior (6.25%), and anterior (6.25%) circumference of the fossa ovalis. The septal pouch opened to the left atrium was observed in 51.2% of specimens.

No observations of structures traversing the atrium from atrial wall to interatrial septum were collected during this study (muscle bridges and networks), however in 7.4% of cases, the fossa ovalis was associated with a net-like structure within the limbus of the fossae ovalis (Fig. 2d). Fig. 2 shows four variations of observed fossa ovalis anatomy: "smooth" fossa ovalis, PFO, RSP and net-like formation within the fossa ovalis. The interatrial septum wall was always the thinnest in the fossa ovalis area (especially in its superior part). The translumination of the fossa ovalis floor did not reveal any difference in its thickness and translucency among four named groups. No interatrial septal aneurysms and atrial septal defects were observed.

4. Discussion

Speaking about the interatrial septum we need to realize the existence of two different, often mistaken, concepts: atrial septum and the true (clinically significant) interatrial septum. The difference between these two concepts is huge. Traditionally comprehended, the interatrial septum represents an extensive area of musculature interposed between the two atria and is bounded as follows: inferiorly by the IVC ostium, antero-inferiorly by the coronary sinus orifice, anteriorly by the right atrioventricular ring (septal leaflet), antero-superiorly by the non-coronary sinus of Valsalva, superiorly by the SVC ostium, and finally posteriorly by folds of the atrial wall (Sweeney and Rosenquist, 1979). This area appears extensive at first sight and could be called a "false" interatrial septum, since transections and dissections reveal that very little part of the aforementioned area can be removed without opening the right atrial wall and arriving outside the heart (Anderson and Brown, 1996).

The true interatrial septum is a relatively small area that could be resected without leaving the cavities of the heart (about 20% of the "false" interatrial septum area). In fact, only the floor of the fossa ovalis and its immediate muscular infero-anterior rim build the septum between the right and left atrium (stippled area in the Fig. 1). When we are looking from the right atrial site, the fossa ovalis has a floor (derived from the septum primum), surrounded by rims. The superior, anterosuperior and posterior rims are formed by infoldings of the adjacent right and left atrial walls and incorporates extracardiac adipose tissue. These rims do not constitute a true interatrial septum, because puncture at these points leads to damage to the outer wall of the heart (Anderson et al., 1999). On the other hand, the infero-anterior rim is a true muscular septum produced by muscularization of the vestibular spine (Anderson et al., 2002). The so-called "septum secundum" is no more that the infolding of the atrial roof between the attachments of the IVC and SVC to the right atrium, and the right pulmonary veins to the left atrium. The true "septum secundum" could be defined as the antero-inferior buttress, which binds the septum to the insulating plane of the atrioventricular junctions.

Despite the great clinical significance, detailed morphology of the true interatrial septum and its dimensions in the adult with no congenital heart diseases has received comparatively little attention. This lack of comprehensive anatomical studies has allowed us to assume proper dimensions and location. We first provided a detailed map of the true interatrial septum detailing the fossa ovalis location in the right atrium with respect to the following main anatomical structures: IVC ostium, right atrioventricular ring, right atrium roof (or SVC ostium). It is interesting and counterintuitive that all dimensions obtained in our study were not associated with gender. This may indicate that the anatomical differences between women and men are increasingly blurred. Further, we noticed the repeated associations between larger measured dimensions and age or heart and body weight.

The PFO is persistence of the foetal interatrial connection at the site of the embryonic ostium secundum. Physiologically during fetal life, the communication is open and closes within the first 2 years of life (Anderson et al., 2002). In approximately 10–35% of adults, a nonadherent flap valve of the septum and the rims of the oval fossa form a small channel across the interatrial septum known as patent foramen ovale (Fisher et al., 1995; Reig et al., 1997). The condition known as a septal pouch occurs when the PFO is absent, but the small pocket within interatrial septum could be shown (Krishnan and Salazar, 2010). The presence of the RSP is undesirable as the RSP may imitate the PFO channel. Additional caution should be taken during manipulation of septal pouch. Due to the nature of the thin wall, slight excessive force even by blunt catheter may cause damage to the tissue. Close proximity of the aortic root to the RSP creates complications as excessive force while guiding catheter through the septal pouch may damage the aortic sinus and associated structures. The PFO channel and RSP may also provide difficulty when accessing inferior pulmonary veins, primarily the right inferior, and the postero-inferior mitral annulus by catheterization due to their locations within septum. However, new deflectable and steerable catheters can mostly eliminate these difficulties.

The net-like structures which we observed within the fossa ovalis in 7.4% of cases (Fig. 2d) can be of embryonic origin, resulting from incomplete overlap and atrophy of different interatrial septum components. We should point out that the observed structures are not the same things as the Chiari's networks. By definition, the Chiari's network is a mobile, net-like structure originating from the Eustachian or Thebesian valve with attachments to the interatrial septum or crista terminalis (Bhatnagar et al., 2006), and the structures that we have seen were limited only to the fossa ovalis area. The presence of net-like structures could hamper the transseptal puncture and further catheter manipulations. The well-developed network could form an additional obstacle on the way to the true septum. Clinically, it could be seen as a bilaminated interatrial septum, represented by a twofold line of the interatrial septum wall, with a contrast layer inside.

The PFO closure is widely used, relatively safe medical procedure (Meier, 2005). However, tunnel-like PFO with a channel length greater than 12 mm create complications and standard closure procedures implemented through the PFO are could be unsuccessful. In our study, we confirm the fact that the PFO appears to disappear with age (Hagen et al., 1984). Based on our many observations, we can conclude that the evolution of the interatrial septum is a continuous, lifelong process, during which the PFO close to form a septal pouch, then a smooth septum.

Transesophageal echocardiography provides an accurate picture of the interatrial septum anatomy and is very useful in planning and conducting transseptal puncture procedures. Results of echocardiographic and cadaver studies on interatrial septum anatomy are consistent (Mesihović-Dinarević et al., 2012; Schwinger et al., 1990). While *in vivo* observation of interatrial septum anatomy is still underdeveloped, recent developments have led to real-time three-dimensional transesophageal echocardiography providing cardiac images, which has proven beneficial to clinicians (Faletra et al., 2011). Moreover, intracardiac echocardiography can provide similar anatomical views that might replace the use of TEE for transseptal procedures (Hijazi et al., 2001). Multidetector computed tomography also comes with the help, as it could provide detailed anatomic information regarding the size, location and morphologic features of the fossa ovalis and its surroundings (Saremi and Krishnan, 2007).

Our main limitation is that all the measurements were made on autopsied heart specimens after formalin fixation, which may result in slight changes in size and shape of the heart. Studies performed on post-mortem material may not directly correlate with the physiology of the tissues *in vivo*. Therefore, we cannot conclude anything about the behavior and dimension changes of the interatrial septum within the cardiac cycle. Despite these limitations, we believe that they do not impede the morphological analysis of relationships between individual heart structures and their relative dimensions.

5. Conclusions

The anatomical map of the interatrial septum from the right atrial side was presented. The RSP may imitate the PFO channel. The "true" interatrial septum represents only about 20% of the whole interatrial septum area. Four different types of the fossa ovalis area could be distinguished.

Conflicts of interest

None.

Appendix A. Supplementary data

Supplementary data associated with this article can be found, in the online version, at http://dx.doi.org/10.1016/j.aanat.2016.01.009.

References

Anderson, R.H., Brown, N.A., 1996. The anatomy of the heart revisited. Anat. Rec. 246, 1–7.
Anderson, R.H., Brown, N.A., Webb, S., 2002. Development and structure of the atrial septum. Heart 88, 104–110.
Anderson, R.H., Webb, S., Brown, N.A., 1999. Clinical anatomy of the atrial septum with reference to its developmental components. Clin. Anat. 12, 362–374.

Bhatnagar, K.P., Nettleton, G.S., Campbell, F.R., Wagner, C.E., Kuwabara, N., Muresian, H., 2006. Chiari anomalies in the human right atrium. Clin. Anat. 19, 510–516.
Bjork, V.O., Malmstrom, G., Uggla, L.G., 1953. Left auricular pressure measurements in man. Ann. Surg. 138, 718–725.
Brock, R., Milstein, B.B., Ross, D.N., 1956. Percutaneous left ventricular puncture in the assessment of aortic stenosis. Thorax 11, 163–171.
Brockenbrough, E.C., Braunwald, E., Ross, J., 1962. Transseptal left heart catheterization. A review of 450 studies and description of an improved technic. Circulation 25, 15–21.
Earley, M.J., 2009. How to perform a transseptal puncture. Heart 95, 85–92.
Facquet, J., Lemoine, J.M., Alhomme, P., Lefebvre, J., 1952. [Transbronchial measurement of left auricular pressure]. Arch. Mal. Coeur Vaiss. 45, 741–745.
Faletra, F.F., Nucifora, G., Ho, S.Y., 2011. Imaging the atrial septum using real-time three-dimensional transesophageal echocardiography: technical tips, normal anatomy, and its role in transseptal puncture. J. Am. Soc. Echocardiog. 24, 593–599.
Fisher, D.C., Fisher, E.A., Budd, J.H., Rosen, S.E., Goldman, M.E., 1995. The incidence of patent foramen ovale in 1,000 consecutive patients. A contrast transesophageal echocardiography study. Chest 107, 1504–1509.
Hagen, P.T., Scholz, D.G., Edwards, W.D., 1984. Incidence and size of patent foramen ovale during the first 10 decades of life: an autopsy study of 965 normal hearts. Mayo Clin. Proc. 59, 17–20.
Hijazi, Z., Wang, Z., Cao, Q., Koenig, P., Waight, D., Lang, R., 2001. Transcatheter closure of atrial septal defects and patent foramen ovale under intracardiac echocardiographic guidance: feasibility and comparison with transesophageal echocardiography. Catheter Cardiovasc. Interv. 52, 194–199.
Jönsson, A., Settergren, M., 2010. MitraClip catheter-based mitral valve repair system. Expert Rev. Med. Devices 7, 439–447.
Katritsis, G.D., Siontis, G.C., Giazitzoglou, E., Fragakis, N., Katritsis, D.G., 2013. Complications of transseptal catheterization for different cardiac procedures. Int. J. Cardiol. 168, 5352–5354.
Krishnan, S.C., Salazar, M., 2010. Septal pouch in the left atrium: a new anatomical entity with potential for embolic complications. JACC Cardiovasc. Interv. 3, 98–104.
Meier, B., 2005. Closure of patent foramen ovale: technique, pitfalls, complications, and follow up. Heart 91, 444–448.
Mesihović-Dinarević, S., Begić, Z., Halimić, M., Kadić, A., Gojak, R., 2012. The reliability of transthoracic and transesophageal echocardiography in predicting the size of atrial septal defect. Acta Med. Acad. 41, 145–153.
Mullins, C.E., 1983. Transseptal left heart catheterization: experience with a new technique in 520 pediatric and adult patients. Pediatr. Cardiol. 4, 239–245.
Radner, S., 1954. Suprasternal puncture of the left atrium for flow studies. Acta Med. Scand. 148, 57–60.
Reig, J., Mirapeix, R., Jornet, A., Petit, M., 1997. Morphologic characteristics of the fossa ovalis as an anatomic basis for transseptal catheterization. Surg. Radiol. Anat. 19, 279–282.
Ross, J., Braunwald, E., Morrow, A., 1960. Left heart catheterization by the transseptal route. A description of the technic and its applications. Circulation XXII, 927–934.
Saremi, F., Krishnan, S., 2007. Cardiac conduction system: anatomic landmarks relevant to interventional electrophysiologic techniques demonstrated with 64-detector CT. Radiographics 27, 1539–1565, discussion 1566-1537.
Schwinger, M.E., Gindea, A.J., Freedberg, R.S., Kronzon, I., 1990. The anatomy of the interatrial septum: a transesophageal echocardiographic study. Am. Heart J. 119, 1401–1405.
Sweeney, L.J., Rosenquist, G.C., 1979. The normal anatomy of the atrial septum in the human heart. Am. Heart J. 98, 194–199.
Zimmerman, H.A., Scott, R.W., Becker, N.O., 1950. Catheterization of the left side of the heart in man. Circulation 1, 357–359.